J. Gen. Appl. Microbiol., **65**, 111–120 (2019)
doi 10.2323/jgam.2018.07.001

jGAM

Full Paper

Salt stress increases carotenoid production of *Sporidiobolus pararoseus* NGR via torulene biosynthetic pathway

(Received May 19, 2018; Accepted July 2, 2018; J-STAGE Advance publication date: November 29, 2018)

Chunji Li,[1] Bingxue Li,[1,*] Ning Zhang,[2] Na Wei,[1] Qifan Wang,[1] Wenjing Wang,[1] Yiwei Xie,[2] and Hongtao Zou[1,*]

[1] *College of Land and Environment, Shenyang Agricultural University, Shenyang 110866, People's Republic of China*
[2] *College of Bioscience and Biotechnology, Shenyang Agricultural University, Shenyang 110866, People's Republic of China*

Carotenoids represent a diverse class of aliphatic C40 molecules with a variety of applications in the food and pharmaceutical industries. *Sporidiobolus pararoseus* NGR produces various carotenoids, including torulene, torularhodin and β-carotene. Salt stress significantly increases the torulene accumulation of *S. pararoseus* NGR. However, little is known, about the molecular mechanisms underlying the increased torulene biosynthesis. In this work, we investigated the effects of NaCl treatment on the contents of carotenoids (both qualitatively and quantitatively) and transcriptome. A total of 12.3 Gb of clean bases were generated in six cDNA libraries. These bases were *de novo* assembled into 9,533 unigenes with an average length of 1,654 nt and N50 of 2,371 nt. Transcriptome analysis revealed that of 3,849 differential expressed genes (DEGs) in response to salt stress, 2,019 were up-regulated, and 1,830 were down-regulated. Among these DEGs, we identified three carotenogenic genes *crtE*, *crtYB*, and *crtI*. In addition, fourteen candidate genes were predicted to participate in the conversion from torulene to torularhodin. Our findings should provide insights into the mechanisms of carotenoid biosynthesis and salt-tolerance of *S. pararoseus* NGR.

Key Words: carotenoids; NaCl; salt-tolerance; *Sporidiobolus pararoseus* NGR; torulene; transcriptome

Introduction

Carotenoids are a group of natural tetraterpenoid pigments primarily found in bacteria, fungi, algae and plants (Maiani et al., 2009). Carotenoids play essential roles in light harvesting, photoprotection and reducing oxidative stress damage in these organisms (Cazzonelli and Pogson, 2010). Carotenoids are divided into two main classes according to their structural features: carotenes and xanthophylls (Müller et al., 2011). Carotenoids are important nutraceuticals because of their known beneficial effects including anti-cancer, anti-aging, anti-inflammatory, anti-angiogenic, cardiovascular protective, and hepato-protective properties (Cazzonelli, 2011). Versatile biological activities of these carotenoids have been attributed to their ability of scavenging free radicals, quenching reactive oxygen species (ROS) and augmentation of self-defense systems (Agarwal et al., 2012; Domonkos et al., 2013). Due to their health-promoting characteristics, carotenoids are used in the cosmetic, pharmaceutical, and food industries (Mata-Gomez et al., 2014). Given these beneficial properties, carotenoids are receiving increasing commercial interest as an alternative natural food additive (Frengova and Beshkova, 2009).

To date, approximately 750 naturally occurring carotenoids have been documented; of which β-carotene, lutein, lycopene and astaxanthin belong to the class of nutraceutical carotenoids (Zuluaga et al., 2017). Torulene is one of the principal carotenoids in *Sporidiobolus pararoseus* and with relatively few studies (Kot et al., 2018). Torulene also is a widespread carotenoid and has a similar molecular structure to lycopene and β-carotene.

*Corresponding authors: Bingxue Li and Hongtao Zou, College of Land and Environment, Shenyang Agricultural University, Shenyang 110866, People's Republic of China.
Tel: +86-13080722022 Fax: +86-24-88487155 E-mail: libingxue1027@163.com (B. Li); zouhongtao2001@163.com (H. Zou)

None of the authors of this manuscript has any financial or personal relationship with other people or organizations that could inappropriately influence their work.

Toxicity studies conducted on rats suggested that torulene produced by red yeast *Rhodotorula glutinis* represents a safe food additive (Latha and Jeevaratanm, 2012). Moreover, recent advances on the biological properties of carotenoids have shown that torulene plays an important role in inhibiting cell growth of human prostate cancer (Du et al., 2016, 2017). Considering that torulene represents a greater potential in the pharmaceutical and food industries, achieving an industrial production has become more and more important (Zoz et al., 2015).

Compared with plants, microorganisms offer a number of advantages as a natural source for large-scale carotenoid production, including high growth rates, continuous growth independent of seasons, and being unrestricted by environmental factors. Oleaginous red yeast is currently attracting considerable attention as a potential renewable source of carotenoids, because of its ability to synthesize mixtures of carotenoids from low-cost carbon sources (Saenge et al., 2011). As one of the oleaginous red yeasts, *S. pararoseus* possesses the potential to grow and synthesize torulene on an industrial scale (Mannazzu et al., 2015). Our work has previously verified that high concentration NaCl significantly increased torulene yield in *S. pararoseus* NGR. The overproduction of torulene and the subsequent quenching of ROS are likely to be a survival mechanism generated in response to salt stress (Li et al., 2017a). However, the molecular mechanism underlying the increased torulene yield in *S. pararoseus* NGR under a high concentration of NaCl has not been fully documented.

Prior to advancements in this field, researchers mainly focused on the production of β-carotene, torulene and torularhodin in *S. pararoseus* using fermentation (Manowattana et al., 2017). Few studies have been conducted on investigating carotenoid production in *S. pararoseus* at the transcriptome level. In the absence of a complete genome sequence in *S. pararoseus*, transcriptomic analysis is an effective method for gaining insights into differentially expressed genes (DEGs) upon exposure to an environmental stress such as an increase in salinity (Mutz et al., 2013). Transcriptome sequencing has been used to identify pathways and genes crucial for biofuel production and the molecular mechanism of secondary metabolite accumulation (Grabherr et al., 2011). Various studies have investigated the related transcript of salt tolerance and carotenoid production in response to various environmental stresses (Udomchalothorn et al., 2017). Here, we set out to investigate the gene expression profiles of *S. pararoseus* NGR under salt stress using transcriptome sequencing.

Materials and Methods

Microbiological material and cultural conditions. *S. pararoseus* NGR was isolated from strawberries. Its strain number is recorded in the China General Microbiological Culture Collection Center as CGMCC 2.5280. Cultures were prepared in 250 mL Erlenmeyer baffle flasks containing 50 mL of the YPD medium (10 g/L yeast extract, 20 g/L peptone and 20 g/L glucose). After inoculation with the pre-cultured cell suspension of *S. pararoseus* NGR, cultures were transferred into flasks and incubated at 28°C on a rotary shaker at 180 rpm. For salt stress experiments, cells were grown in YPD medium under optimized conditions (28°C, 180 rpm and pH 6.5) with initial NaCl concentrations of 0.75 M throughout 3 days of growth period. All experiments were carried out in triplicates in 250 mL flasks containing 50 mL of respective culture medium and inoculated with 1% (v/v) of actively growing culture of *S. pararoseus* NGR (OD_{500} = 0.02). The final optical densities (OD_{500}) attain 15.8 after salt stress of 3 days of cultivation.

Total RNA extraction and cDNA library construction. The total RNA was isolated from six samples using Trizol reagent kit (Invitrogen, USA) according to the manufacturer's instructions. RNA samples were treated with RNase-free Dnase I to avoid DNA containment. RNA contamination and degradation were checked using 1% agarose gel electrophoresis. RNA purity was checked with a Nano Photometer spectrophotometer (IMPLEN, USA). Qubit RNA Assay Kit and Qubit 2.0 Flurometer (Life Technologies, USA) were used to measure RNA concentration. RNA Nano 6000 Assay Kit and Agilent Bioanalyzer 2100 system (Agilent Technologies, USA) were used to assess the RNA integrity of each sample. A total amount of 3 μg RNA per sample was used as input material for RNA sample preparations. Sequencing libraries were generated by NEB Next Ultra RNA Library Prep Kit (NEB, USA) following the manufacturer's protocol. Index codes were added to attribute sequences to each sample. Briefly, mRNA was purified from the total RNA using poly-T oligo-attached magnetic beads. Fragmentation was accomplished using divalent cations under elevated temperature in NEB Next First Strand Synthesis Reaction Buffer (5X). First strand cDNA was synthesized using random hexamer primer and M-MuLV Reverse Transcriptase (RNase H^-). Second strand cDNA synthesis was subsequently performed using DNA polymerase I and RNase H. The remaining overhangs were converted into blunt ends via exonuclease/polymerase activities. After adenylation of 3′ ends of DNA fragments, NEB Next Adaptor with a hairpin loop structure were ligated to prepare for hybridization. In order to select cDNA fragments of preferentially 150~200 bp in length, the library fragments were purified with AMPure XP system (Beckman Coulter, USA). Next, 3 μL USER Enzyme (NEB, USA) was used with size-selected, adaptor-ligated cDNA at 37°C for 15 min followed by 5 min at 95°C before PCR. PCR was then executed with Phusion High-Fidelity DNA polymerase, Universal PCR primers and Index (X) Primer. Finally, PCR products were purified (AMPure XP system) and library quality was assessed on the Agilent Bioanalyzer 2100 system (Agilent Technologies, USA) (Bi et al., 2018).

Sequence assembly and annotation. Raw reads generated by Illumina HiSeq 2000 were processed to obtain clean reads by removing adaptor sequences, reads containing poly-N and low quality reads through in-house perl scripts (Gong et al., 2015; Shen et al., 2017). Q20, Q30, GC-content and the sequence duplication level of the clean data were calculated. Clean reads were randomly clipped into short fragments (K-mers) by applying Trinity program (Grabherr et al., 2011). The K-mers with a certain length

of overlap were combined to form longer fragments and contigs. The overlap between these contigs was utilized to build graph components. The clean reads were then mapped back onto the assembled transcriptome using the method of the De Bruijn graph. Finally, the unique assembled transcriptome were further subjected to the process of sequences-splicing redundancy removal using TIGR gene indices clustering tools to acquire non-redundant transcripts called unigenes (Martin and Wang, 2011).

cDNA sequences of unigenes were aligned to the Nr database (NCBI non-redundant protein sequences) via blastx (v 2.2.28, *E*-value ≤ 1×10^{-5}). Information of the top 10 hits of each unigene in Nr was extracted through an in-house script. Blasting against NT database (NCBI non-redundant nucleotide sequence) was performed using blastn. Annotation in Pfam (Protein family) database and Swiss-Prot (A manually annotated and reviewed protein sequence database) were performed using hmmscan. Annotation in KOG/COG (Clusters of Orthologous Group of protein) was performed via blastx. Functional GO annotation was performed using the blast2GO program (v3.0). Metabolic pathway analysis was carried out through mapping unigenes to the KEGG database via KEGG Automatic Annotation Server (KAAS). Unique KO IDs encoded by Sepia unigenes were extracted and submitted to iPath v2, with the edge width standing for the frequency of each KO IDs (edge width= $\log_2$ (Frequency+1) × 5). When a unigene failed to align to any of the above databases, the ESTScan software (3.0.3) was introduced to predict the coding regions fragment (ORF) and determine the direction of the sequence (Iseli et al., 1999).

Differential gene expression analysis. Raw data of DGE sequencing were filtered using a perl script. DGEs analysis was biologically replicated three times. Expression levels of unigenes were estimated using RSEM (Li and Dewey, 2011). Clean data were mapped back onto the assembled transcriptome. Readcount for each gene was obtained from these mapping results. Expression profiling was carried out based on FPKM. To identify differentially expressed genes across samples, the edgeR package (www.r-project.org/) was used (Robinson et al., 2009). Differential expression analysis of two group samples was performed using the DEGseq R package (v1.10.1) (Anders and Huber, 2010). The resulting *P*-values were adjusted using Benjamini and Hochberg's approach for controlling the false discovery rate (Li et al., 2017b). Genes with an adjusted *P*-value < 0.05 (Padj) were considered differentially expressed. The confirmed DGEs were subjected to GO functional enrichment analysis and KEGG pathway analysis (Rapaport et al., 2013). The DEGs identified as being involved in carotenoid biosynthesis and salt-tolerance were used for further analysis. Detailed programs information used in this transcriptome analysis is listed as Table S1.

Quantitative real-time PCR. Total RNA was extracted using the Yeast RNAiso Kit (Takara, Japan), the RNA was digested with Recombinant DNase I (RNase-free) (Takara, Japan). The digested RNA was used for cDNA synthesis using the M-MLV Rtase cDNA Synthesis Kit (Takara, Japan). Quantitative real-time PCR was performed in a StepOne Plus System (Applied Biosystems, USA) using the SYBR Premix Ex *Taq*II Kit (Takara, Japan) according to the manufacturer's protocol. Primers used are listed in Table 1. A 20 μL PCR system was prepared that contained 2 μL cDNA templates, 0.8 μL of each primer (0.4 μM), 10 μL SYBR Premix Ex *Taq*II, 0.4 μL ROX Reference Dye (50×) and 6 μL RNase-free water. As a negative control, template DNA was replaced by PCR-grade water. The specificity of the amplified PCR product was identified by performing melting curve analysis using a StepOne Plus system (Applied Biosystems, USA). The 26S rDNA was selected as an internal reference. For analysis of the quantitative results, the relative expression of each gene was calculated by the comparative crossing point (CP) method and presented as $2^{-\Delta\Delta Ct}$. Each gene expression analysis was performed with three independent biological replicates.

Table 1. Oligonucleotide primers in this study.

Primer name	Sequence (5′-3′)
26S-F	AGCGGAGGAAAAGAAACTAACA
26S-R	TGCGGTCTATCACGGAAAAC
crtE-F	TGTCGCTCACAAGATTTACGG
crtE-R	CAAAAGTTCCTGTGTGACCATCT
crtI-F	AGTCATCACGGAAAGTGGAGAA
crtI-R	ATAGCCCAAACCAGGTCAGC
crtYB-F	GAATCAACCCGATACGAAACA
crtYB-R	TAATCTCAAGCGACCATCAAAC

Extraction and high performance liquid chromatography (HPLC) analysis of carotenoids. Strains were grown for 3 days under dark conditions to avoid pigment degradation, and cells were collected by centrifugation at 3,000 × *g*, and were washed twice with sterile water. Following freeze-drying of the washed cells, carotenoids were soaked in DMSO-acetone (1/3, v/v), vigorously vortexed and incubated for 30 min in a water bath at 65°C. Following a centrifugation step as described above, the supernatant containing carotenoids were transferred into a new tube, and the extraction was repeated until the thallus became colorless (Buzzini et al., 2005). All operations were performed under dark conditions to limit carotenoids degradation. Pigment extracts were stored in sealed vials under nitrogen gas and stored at –20°C until further use. All samples were filtered through 0.45 μm microporous film before injections.

HPLC analysis of carotenoids was carried out on a CBM-20A system with SPD-M20A diode array detector (Shimadzu, Japan). Carotenoids were separated on a reverse-phase column (C18, 5 μm, 250 × 4.6 mm, Dikma Diamonsil (2), USA) by gradient elution with a mobile phase of acetonitrile and H_2O (9:1, v/v) as eluent A, and ethyl acetate as eluent B. A gradient program was executed: 0–6 min, 20–60% B; 6–15 min, 60% B; 15–20 min, 60–100% B; 20–25 min, 100–20% B; 25–30 min, 20% B isocratic step. The UV-visible absorption spectra were recorded at 450 nm, and the flow rate was fixed at 1 mL/min according to a previous report (Weber et al., 2007). A sample of β-carotene standard was used to prepare a 6-point calibration curve at 450 nm with R^2 = 0.9969. Torulene, torularhodin, and β-carotene were quantified against peak area calibration calculated from β-carotene

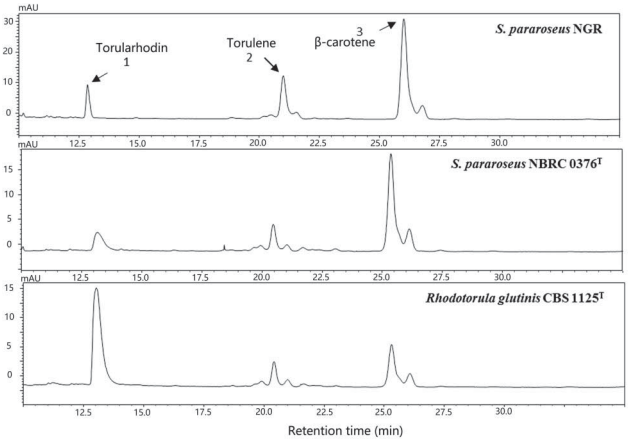

Fig. 1. HPLC profiles of carotenoids produced by the *S. pararoseus* NGR strain using the exemplary chromatograms of the carotenoids produced by standard strain *S. pararoseus* NBRC 0376^T and *Rhodotorula glutinis* CBS 1125^T.

The following carotenoids were identified: peak 1: torularhodin; peak 2: torulene; peak 3: β-carotene.

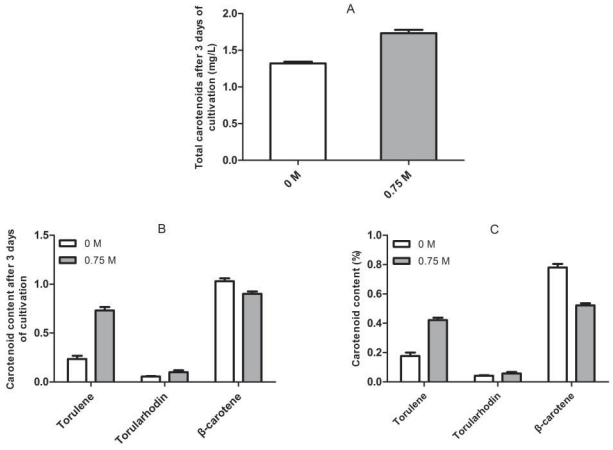

Fig. 2. Individual carotenoid content and composition (w/v) of *S. pararoseus* NGR were measured under 0.75M NaCl treatments and control.

A. The total carotenoids after 3 days of cultivation with NaCl and control; B. Torulene, torularhodin and β-carotene yield after 3 days of cultivation with NaCl and control, respectively; C. Torulene, torularhodin and β-carotene percentage of total carotenoids after 3 days of cultivation with NaCl and control, respectively; Error bars represent the standard deviation. Different letters indicate statistically significant difference. The data analysis was performed using the software package SPSS 19.0 of Windows.

standard curves according to a previous report (Buzzini et al., 2007), due to the unavailable of commercial standards of torulene and torularhodin. The column temperature was 25°C, and the injection volume for each sample was 20 μL. Carotenoid analysis was performed in three independent biological replicates. The β-carotene standard substance was purchased from Sigma-Aldrich (St. Louis, MO, USA).

Statistical analysis. The data of various physiological indices in Fig. 2 were analyzed using the software package SPSS 19.0 of Windows (SPSS Inc., USA). Prior to analysis, data were normalized by transforming as ln(x+1). All data were expressed as means ± standard error of at least triplicates of independent cultures. The means of different treatments were compared by one-way ANOVA using Turkey's honestly significant difference test at the 5% probability level ($p < 0.05$).

Table 2. Summary of annotations of the *S. pararoseus* NGR.

	Number of Unigens	Percentage (%)
Annotated in NR	6103	64.01
Annotated in NT	604	6.33
Annotated in KO	2406	25.23
Annotated in SwissProt	4578	48.02
Annotated in PFAM	5305	55.64
Annotated in GO	5456	57.23
Annotated in KOG	3778	39.63
Annotated in all Databases	441	4.62
Annotated in at least one Database	6826	71.6
Total Unigenes	9533	100

NR: NCBI non-redundant protein database; *NT*: NCBI nucleotide database; *SwissProt*: SwissProt protein database; *PFAM*: PFAM protein database; *GO*: Gene Ontology database; *KOG*: euKaryotic Ortholog Groups database.

Results and Discussion

Effect of NaCl treatment on carotenoids content

As shown in Fig. 1, *S. pararoseus* NGR mainly accumulates β-carotene, torulene and torularhodin. Our previous study showed that 0.75 M is an appropriate concentration for increasing carotenoid yield of *S. pararoseus* NGR. In order to identify the effect of 0.75 M NaCl treatment on carotenoid production, we used HPLC analysis. As shown in Fig. 2A, after 3 days of cultivation, the total amount of carotenoids was significantly higher in the salt treated cultures (1.73 mg/L) compared with the control (0 M) (1.32 mg/L). As shown in Fig. 2B, after 3 days of cultivation, torulene production was significantly higher under salt stress (0.73 mg/L) compared with the control cultures (0.23 mg/L), with a 2.17-fold increase. As shown in Fig. 2C, the relative proportion of torulene increased to approx. 40% under salt stress conditions relative to salt-free conditions (approx. 18%). Moreover, after 3 days of cultivation, compared with the control (0.0558 mg/L), the torularhodin production of NaCl treatment (0.0998 mg/L) increased by 79.0%. The percentage of torularhodin of total carotinoids increased by 1.53% (control: 4.23% and salt treated cultures: 5.76%). In contrast, β-carotene production decreased by 12.42% to a level of 0.9 mg/L under salt stress conditions. Together our results show that torulene accumulation is a major contributor to the total carotenoid yield under salt stress. Salt stress usually increases the level of intracellular reactive oxygen species (ROS) (Ben Rejeb et al., 2015; Miller et al., 2010). The protection of cells against ROS, realized by the quenching of singlet oxygen molecules as well as by the scavenging of free radicals, is one of the main biological functions of carotenoids (Domonkos et al., 2013). To protect themselves against the adverse effects of high salt conditions, cells produce more torulene, which quenches ROS. In comparison, increased torularhodin accumulation is likely to result from the increasing precursor torulene pro-

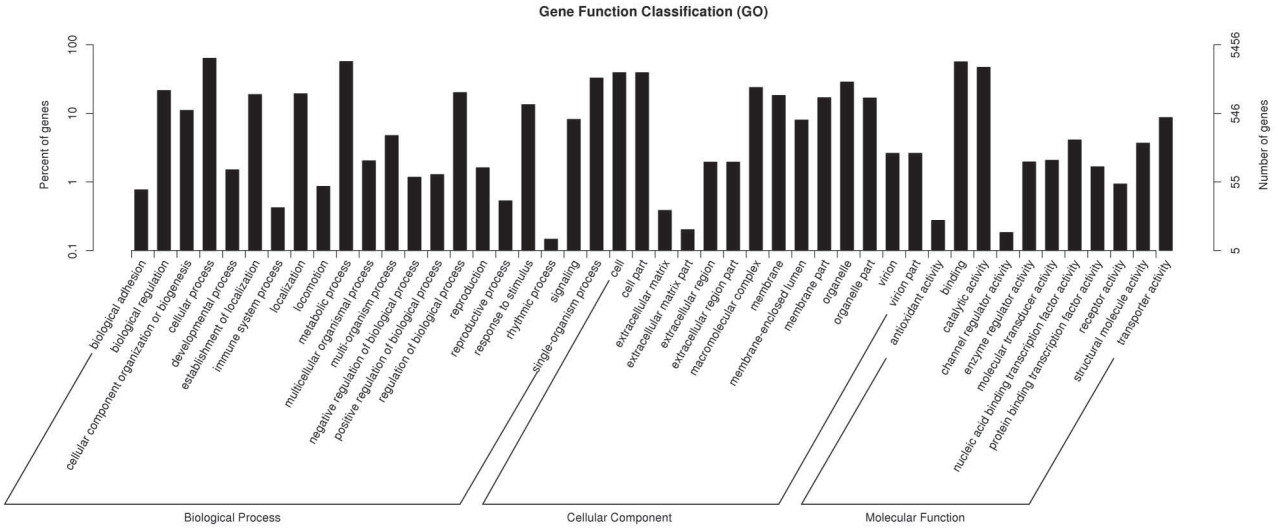

Fig. 3. Gene ontology (GO) classification of all assembled unigenes of the *S. pararoseus* NGR transcriptome.

The assembled unigenes mapped to three main categories: biological process, cellular component and molecular function. The *x*-axis represents GO terms and the *y*-axis shows the number of the matching unigenes in a category.

duction, and probably plays little or no function in protecting against ROS.

Illumina sequencing and De novo transcriptome assembly

In order to understand how torulene production is activated, we compared their transcriptome characteristics performing transcriptome sequencing, using total RNA prepared from strains with NaCl treatment and control. Sequencing of cDNA libraries of both salt and salt-free samples generated a total of 27,660,545 and 23,478,289 raw reads, respectively. After removing the adaptor sequences, low-quality reads, and ambiguous reads, 27,289,439 and 23,165,064 single-end clean reads (Q20 > 96%, Q30 > 89%) were obtained for assembly from NaCl treatment and control strains, respectively. The Trinity program (Broad Institute, USA) was used to assemble all clean reads, with a minimum length of 201 nt, a maximum length of 16297 nt, an average length of 1,654 nt, and an N50 of 2,371 nt. We used Bowtie2 software and the DESeq library to estimate expression abundance and obtained 9,533 unigenes. All RNA-seq clean reads were deposited into the NCBI-SRA (SRA accession: SRP131948).

Functional annotation of assembled transcripts

To understand the features and functions of the assembled transcripts, we annotated the assembled transcripts to several public databases, including NCBI non-redundant (NR), Protein Data Bank (PDB), Swiss-Prot, GO and KEGG pathway. The numbers of transcripts aligned to each of the databases are listed in Table 2. Of the total 9,533 transcripts, 6,103 transcripts (64.01%) generated BLAST hits to known proteins in the NR database, as well as 604 transcripts (6.33%) BLAST hits to nucleotides in the NT database. In addition, a large number of transcripts were aligned to public databases, including 4,578 (48.02%) transcripts in the Swiss-Prot protein database, 5,305 (55.64%) transcripts in the PFAM protein database, 2,406 (25.23%) transcripts in the KEGG Ortholog (KO), 3,778 (39.63%) transcripts in the euKaryotic Ortholog Groups (KOG) and 5,456 (57.23%) transcripts in the Gene Ontology (GO). In total, 6,826 transcripts were annotated in at least one database, representing approximately 71.6% of all assembled transcripts. Gene ontology (GO) analysis revealed that 5,456 of the total assembled transcripts were distributed in 46-sub-categories under three main GO functional categories: biological process, cellular components and molecular functions as listed in Fig. 3. GO term distribution of the assembled transcripts showed that the "cellular process" and "metabolic process" were the two most abundantly represented with 3,468 (63.56%) and 3,106 (56.93%) transcripts, respectively. In the "cellular components" ontology transcripts were mainly distributed in "cell" (2145, 39.31%), "cell part" (2144, 39.30%) and "organelle" (1561, 28.61%). GO analysis also showed 3082 (56.49%) transcripts had a "binding" function and 2560 (46.92%) with "catalytic activity" function in the "molecular function" ontology. In addition, some transcripts (4077, 42.77%) showed no similarity to any known protein database, these might be putative long-noncoding RNAs (LncRNA) or novel genes, and future studies are required to identify them.

Identification of differentially expressed genes (DEGs) responding to salt stress

To measure the gene expression profiles, we calculated each sample using the DESeq R package (v1.12.0). A total of 3849 DEGs were found between salt and salt-free libraries, with 2019 up-regulated and 1830 down-regulated genes fulfilling the threshold of q-value < 0.05 and $|\log_2$ fold-change$|$ > 1 (Fig. 4A).To understand the expression

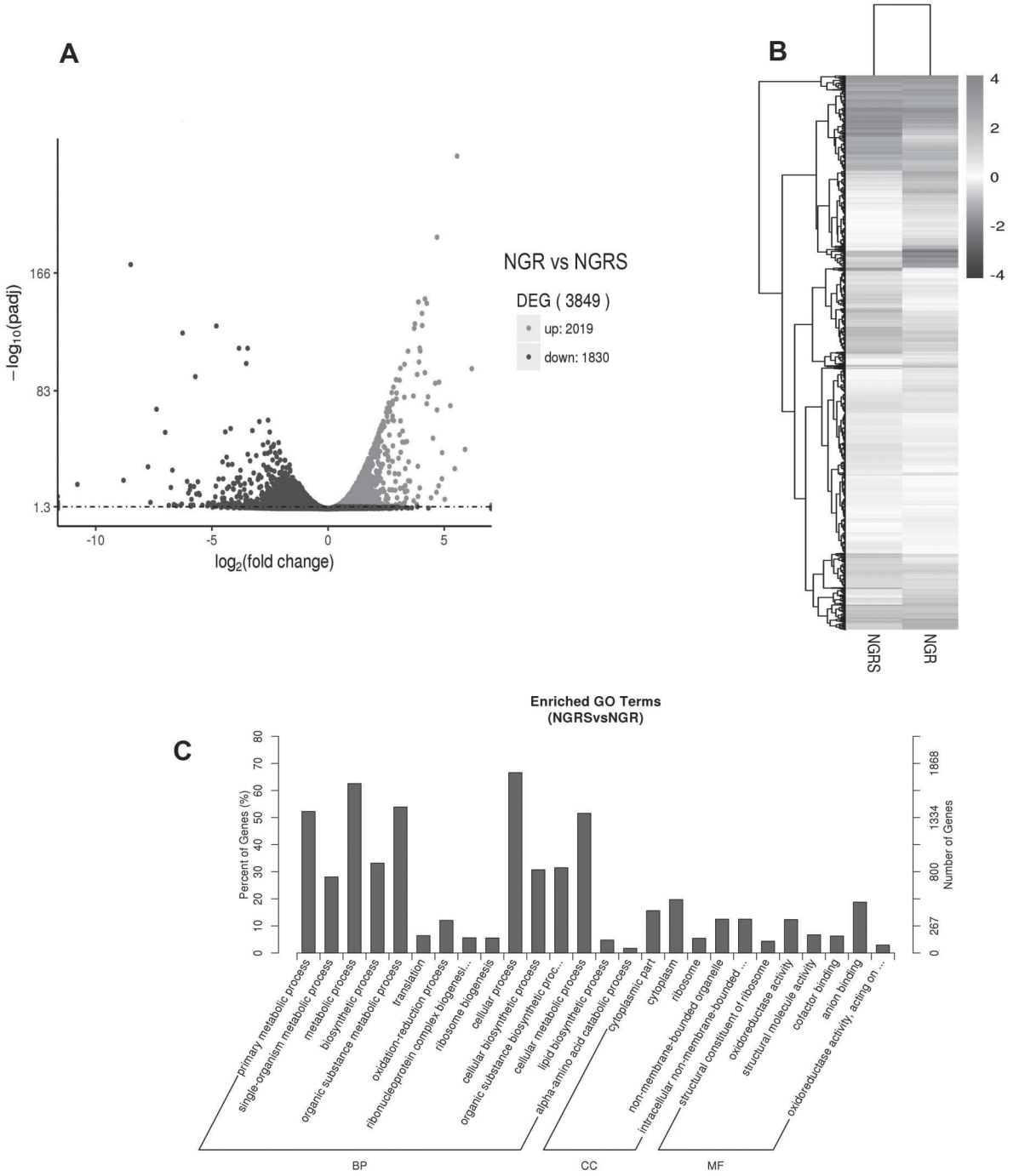

Fig. 4. Transcriptomes analysis of *S. pararoseus* NGR with two comparisons: 0.75M NaCl treatment (NGRS); the control (NGR). A. Volcano plots showing the numbers of DGEs in the two comparisons. Right: up-regulated genes; Left: down-regulated genes; analysis parameter: q-value < 0.05, and $|\log_2$ fold-change$| > 1$; B. Hierarchical cluster analyses of the 3849 DEGs in two comparisons, each column represents a comparison, each row represents a gene. Expressional differences are shown in different colors. Red means up-regulated and blue means down-regulated; C. Comparison of gene ontology (GO) analysis for up- and down-regulated DEGs in response to 0.75M NaCl compared with the control. BP: biological process; CC: cellular component; MF: molecular function. The x-axis represents GO terms and y-axis shows the number of the matching unigenes in a category.

patterns of DEGs, we performed hierarchical clustering analysis based on their FPKM values (Fig. 4B). This result suggested that these overlapping DEGs may play an important role in the response to salt stress. To gain more detailed insights into the functions of DEGs, we performed GO enrichment analysis, using a corrected p-value < 0.05 as the cutoff. As shown in Fig. 4C, a total of 26 GO terms were found to be enriched. Most of these GO terms were associated with a biological process (BP). This result is associated with the phenomenon that environmental stress

Table 3. The candidate genes involved in the biosynthesis from torulene to torularhodin.

Gene classification	Gene number	Predictive genetic function
Hydroxylase	*comp 1142*	fatty acid hydroxylase superfamily
	comp 5151	fatty acid hydroxylase superfamily
	comp6175	leukotriene-B(4) omega-hydroxylase
	comp 9900	cephalosporin hydroxylase
Monooxygenase	*comp 1598*	squalene monooxygenase
	comp 1689	monooxygenase
	comp 2101	monooxygenase
	comp 4759	monooxygenase
	comp 5660	uncharacterized monooxygenase
	comp 6728	monooxygenase
	comp 6823	squalene monooxygenase
Oxidase	*comp 2438*	prenyltransferase and squalene oxidase repeat
	comp 3479	prenyltransferase and squalene oxidase repeat
	comp 4169	prenyltransferase and squalene oxidase repeat

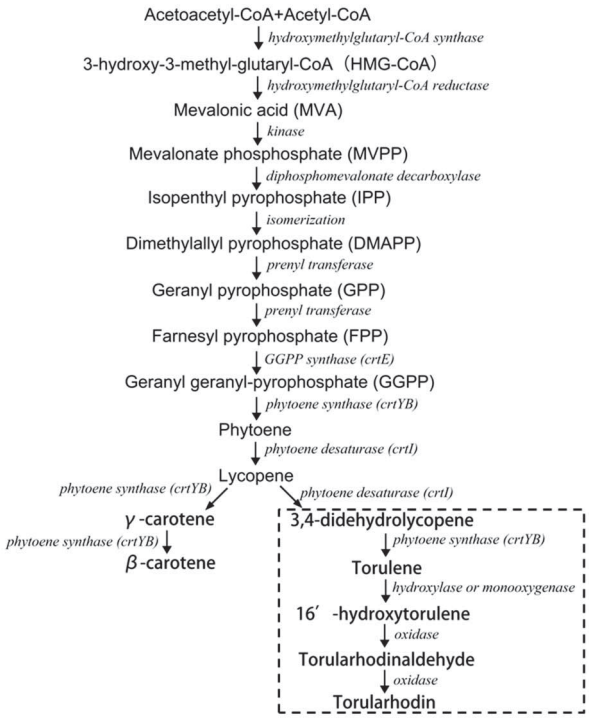

Fig. 5. The proposed carotenogenic pathways from acetyl-CoA to β-carotene, torulene and torularhodin in *S. pararoseus* NGR.

The speculative transformation from 3,4-didehydrolycopene to torularhodin is shown in the dotted box. The corresponding catalytic enzyme name is listed in italics below the substrate.

usually promotes the biosynthesis of some secondary metabolites, such as hormones and pigments (Gill and Tuteja, 2010). Other enriched GO terms were related to oxidoreductase activity, such as oxidoreductase activity and oxidation-reduction process (Liu et al., 2016). Together, these results strongly indicate that oxidoreductase activity is a key element in establishing the tolerance of organism against salt stress. In agreement with our findings here, a previous report showed similar results on the *Achnatherum splendens* in the response to salt stress (Liu et al., 2016). This is likely attributed to the fact that salt stress induces an increase in the intracellular ROS level (Miller et al., 2010).

Table 4. Expression of DEGs in salt-responsive KEGG pathways (NGRS vs NGR).

Salt-tolerance related pathways	Down	Up
Arginine and proline metabolism	14	7
Calcium signaling pathway	6	4
ABC transporters	3	5
Nitrogen metabolism	3	2
Oxidative phosphorylation	12	25
MAPK signaling pathway - yeast	3	10
MAPK signaling pathway	5	11
Glycine, serine and threonine metabolism	13	2
PI3K-Akt signaling pathway	7	11
Starch and sucrose metabolism	2	7
Phosphatidylinositol signaling system	4	2

Analysis of DEGs involved in carotenoid metabolism

Our analysis of the transcriptome of the *S. pararoseus* NGR exposed to salt stress allowed as to guide the identification of a number of genes responsible for the carotenoid biosynthesis (fold-change ≥ 1.2) (Ariotti et al., 2014; Hren et al., 2009). Among these genes, *comp6178* (GGPP synthase, *crtE*, GenBank: KY652916), *comp5921* (lycopene cyclase/phytoene synthase, *crtYB*, GenBank: KR108013) and *comp1804* (phytoene desaturase, *crtI*, GenBank: KR108014) (Li et al., 2016) are directly related to the biosynthesis of torulene, torularhodin and β-carotene. As shown in Fig. 5, the biosynthesis of carotenoids start with the conversion from acetyl-CoA to 3-hydroxy-3-methyl glutaryl-CoA (HMG-CoA), catalyzed by HMG-CoA synthase (Frengova and Beshkova, 2009). Subsequently, HMG-CoA undergoes a series of reactions to form two terpenoid compounds isopentenyl diphosphate (IPP) and dimethylallyl pyrophosphate (DMAPP). The condensation reaction of IPP and DMAPP into geranylgeranyl pyrophosphate (GGPP) is catalyzed by prenyl transferase/GGPP synthase (*crtE*), which was found to be up-regulated 1.59-fold under salt stress. The condensation of two GGPP molecules into phytoene and lycopene into β-carotene are catalyzed by bifunctional lycopene cyclase/phytoene synthase (*crtYB*), which was up-regulated 1.55-fold under salt stress. Our previous results showed that the enzymatic conversion of phytoene to lycopene and 3,4-

didehydrolycopene is catalyzed by this phytoene desaturase (*crtI*) of *S. pararoseus* NGR through consecutive dehydrogenation (Li et al., 2016), which was up-regulated 1.34-fold. Furthermore, 3,4-didehydrolycopene is the precursor of torulene in *Neurospora crassa* and the biological transformation from 3,4-didehydrolycopene to torulene is catalyzed by bifunctional phytoene synthase/lycopene cyclase AL-2 (Sandmann et al., 2006). It has been proposed earlier that torulene is produced from 3,4-dehydrolycopene in both red yeast *Xanthophyllomyces dendrorhous* and *Rhodosporidium toruloides*. On the basis of these results, we hypothesized that the possible pathway of torulene biosynthesis in *S. pararoseus* NGR is from lycopene to 3,4-didehydrolycopene to torulene (Li et al., 2017a). The *crtI* gene up-regulation result in a higher 3,4-didehydrolycopene accumulation and an improvement in the torulene synthesis capacity.

Hydroxylation and oxidation of torulene by mixed function oxidase leads to the formation of torularhodin through the intermediates 16′-hydroxytorulene and torularhodinaldehyde (Herz et al., 2007). Torularhodin, a common end product of carotenoid oxidation in red yeasts, was not produced by either species under any incubation condition (Herz et al., 2007). Torulene and torularhodin have been synthesized by chemical methods. However, so far, the enzymes catalyzing the conversion from torulene to torularhodin in natural sources remain unclear. The conversion from torulene to 16′-hydroxytorulene should be catalyzed by hydroxylase or monooxygenase; and the continuous conversions from 16′-hydroxytorulene to torularhodinaldehyde and torularhodin should be catalyzed by one or more oxidases. Expressions of the related hydroxylase, monooxygenase and oxidase genes are listed in Table 3. Among these hydroxylases and monooxygenases, *comp1598* (hypothesized squalene monooxygenase) and *comp6823* (hypothesized squalene monooxygenase) are the most likely candidate genes to catalyze the transformation from torulene to 16′-hydroxytorulene. Furthermore, we predicted *comp2438*, *comp3479* and *comp4169* process "prenyltransferase and squalene oxidase repeat" feature. On the basis of our analysis, we propose that these three genes convert 16′-hydroxytorulene to torularhodin. However, direct biochemical evidence is required to confirm this assumption.

Analysis DEGs involved in salt-stress tolerance pathways

Even single cell organisms have developed complex gene regulatory networks. One important part of these networks is involved in responding to environmental challenges. For example, salt stress has been shown to activate a cascade of genes regulating the expression of enzymes involved in producing carotenoids to protect against the toxic effects of salt. As shown in Table 4, we found the enriched DEGs involved in these salt-responsive KEGG pathways. Among them, the 'oxidative phosphorylation' pathway contained the highest number of DEGs. This phenomenon also proves that salt stress mainly causes oxidative stress. In addition, a number of DEGs were present in the 'arginine and proline metabolism' sub-groups of 'metabolism' and in the 'PI3K-Akt signaling pathway' sub-groups of signal transduction pathways of 'environmental information processing'. Other researchers have reported similar pathways of salinity stress respond in *Crossostephium chinensis* and Asteraceae halophyte *Karelinia caspica* (Yang et al., 2017; Zhang et al., 2014). This suggests that these pathways are common when organisms response to salt stress. Except for the salt-stress tolerance pathways mentioned above, enhanced carotenoid biosynthesis also is one of the most crucial mechanisms of improved salt-tolerance. Kim et al. reported that increased carotenoid accumulation exhibited a strengthened antioxidant activity and salt-tolerance of transgenic sweetpotato cultures (Kim et al., 2013). Another study reported that the salt-tolerance of *Nicotiana tabacum* is conferred by enhanced carotenoid production, resulting in improved/increased ability to scavenge reactive oxygen species (ROS) (Shi et al., 2015). Kang et al. also observed that increased β-carotene levels significantly enhanced salt-stress tolerance of transgenic sweetpotato (Kang et al., 2017).

In addition, improved tolerance could be achieved by altering expression levels of the existing genes to affect the degree of salt-stress tolerance. Previously, our results suggested that amongst the three carotenoids tested, torulene provides more protection against oxidative stress than torularhodin and β-carotene (Li et al., 2017a). Moreover, torulene has been demonstrated earlier to have a higher relative free radical scavenging activity than β-carotene (Galano and Francisco-Marquez, 2009; Sakaki et al., 2002). Therefore, torulene possesses a bigger potential to improve salt tolerance in salt-tolerant transgenic plants than β-carotene.

Validation of gene expression

To confirm the Illumina sequencing data for genes involved in carotenoids biosynthesis. We tested the mRNA expression of three carotenogenic unigenes including *comp6178* (GGPP synthase, *crtE*), *comp5921* (lycopene cyclase/phytoene synthase, *crtYB*) and *comp1804* (phytoene desaturase, *crtI*) by qPCR. The expression profiles of *comp6178*, *comp5921* and comp1804 were 1.8-fold, 2.5-fold and 3.2-fold, respectively. These results indicated that the three carotenogenic gene expression levels detected by Illumina sequencing analysis at 3d were mostly consistent with the qPCR. This comparison confirmed the reliability of the RNA-seq results.

Conclusion

Here, we employed NGS sequencing to analyze changes in the transcriptome profiling of *S. pararoseus* NGR in response to salt stress. In summary, a total 9533 unigenes from NaCl treatment and control strains have been identified. 6,826 unigenes were annotated in at least one database, representing approx. 71.6% of the total and others may be LncRNA or novel genes. 3849 unigens were expressed differently between NaCl treatment and control strains. Functional enrichment using GO and KEGG annotations showed that these DEGs participate in many important biological and metabolic pathways, including biological process, oxidoreductase activity, carotenoid biosynthesis and salt-stress tolerance. Among them, we

identified three carotenogenic unigenes including *crtE*, *crtYB* and *crtI*, four hydroxylase unigenes, seven monooxygenase unigenes and three oxidase unigenes. These candidate unigenes are likely to be involved in carotenoid biosynthesis. Taken together, our findings should improve the understanding of carotenoid biosynthesis in *S. pararoseus* NGR. Our further studies will focus on genomics, proteomics and metabolomics with regard to achieving the induction and regulation of torulene biosynthesis on an industrial scale.

Acknowledgments

We thank Torsten Juelich (Peking University, China) and Mark Radosevich (University of Tennessee, USA) for linguistic assistance during the manuscript preparation. This work is supported by the National Natural Science Foundation of China (Grant No. 31271818), the National Key Research and Development Program of China (Project No. 2017YFD200807-3), the Natural Science Foundation of Liaoning Province of China (Grant No. 2015020763), and the Shenyang Science and Technology Innovation in Agriculture Special Fund (Grant No. F17-150-3-00).

Author Contributions

Chunji Li performed the experiments, analyzed the data, contributed reagents/materials/analysis tools, and wrote the paper, and prepared the figures and tables. Bingxue Li, Ning Zhang and Hongtao Zou conceived the study design/ideas and the funding acquisition and supervised the whole written procedure. Na Wei provided technological assistance for HPLC analysis. Qifan Wang, Wenjing Wang and Yiwei Xie provided kind assistance for qPCR validation. All authors have read and approved the final manuscript.

Conflicts of Interest

The authors declare that they have no conflict of interests.

Supplementary Materials

Supplementary table is available in our J-STAGE site (http://www.jstage.jst.go.jp/browse/jgam).

References

Agarwal, M., Parameswari, R. P., Vasanthi, H. R., and Das, D. K. (2012) Dynamic action of carotenoids in cardioprotection and maintenance of cardiac health. *Molecules*, **17**, 4755–4769.

Anders, S. and Huber, W. (2010) Differential expression analysis for sequence count data. *Gonome Biol.*, **11**, R106.

Ariotti, S., Hogenbirk, M. A., Dijkgraaf, F. E., Visser, L. L., Hoekstra, M. E. et al. (2014) Skin-resident memory $CD8^+$ T cells trigger a state of tissue-wide pathogen alert. *Science*, **346**, 101–105.

Ben Rejeb, K., Benzarti, M., Debez, A., Bailly, C., Savouré, A., and Abdelly, C. (2015) NADPH oxidase-dependent H_2O_2 production is required for salt-induced antioxidant defense in *Arabidopsis thaliana*. *J. Plant Physiol.*, **174**, 5–15.

Bi, H., Guo, M., Wang, J., Qu, Y., Du, W. et al. (2018) Transcriptome analysis reveals anthocyanin acts as a protectant in *Begonia semperflorens* under low temperature. *Acta Physiol. Plant.*, **40**, 10.

Buzzini, P., Martini, A., Gaetani, M., Turchetti, B., Pagnoni, U. M. et al. (2005) Optimization of carotenoid production by *Rhodotorula graminis* DBVPG 7021 as a function of trace element concentration by means of response surface analysis. *Enzyme Microb. Tech.*, **36**, 687–692.

Buzzini, P., Innocenti, M., Turchetti, B., Libkind, D., van Broock, M. et al. (2007) Carotenoid profiles of yeasts belonging to the genera *Rhodotorula*, *Rhodosporidium*, *Sporobolomyces*, and *Sporidiobolus*. *Can. J. Microbiol.*, **53**, 1024–1031.

Cazzonelli, C. I. (2011) Carotenoids in nature: insights from plants and beyond. *Funct. Plant Biol.*, **38**, 833–847.

Cazzonelli, C. I. and Pogson, B. J. (2010) Source to sink: regulation of carotenoid biosynthesis in plants. *Trends Plant Sci.*, **15**, 266–274.

Domonkos, I., Kis, M., Gombos, Z., and Ughy, B. (2013) Carotenoids, versatile components of oxygenic photosynthesis. *Prog. Lipid Res.*, **52**, 539–561.

Du, C., Li, Y., Guo, Y., Han, M., Zhang, W. et al. (2016) The suppression of torulene and torularhodin treatment on the growth of PC-3 xenograft prostate tumors. *Biochem. Bioph. Res. Co.*, **469**, 1146–1152.

Du, C., Guo, Y., Cheng, Y., Han, M., Zhang, W. et al. (2017) Anti-cancer effects of torulene, isolated from *Sporidiobolus pararoseus*, on human prostate cancer LNCaP and PC-3 cells via a mitochondrial signal pathway and the down-regulation of AR expression. *Rsc Adv.*, **7**, 2466–2474.

Frengova, G. I. and Beshkova, D. M. (2009) Carotenoids from *Rhodotorula* and *Phaffia*: yeasts of biotechnological importance. *J. Ind. Microbiol. Biot.*, **36**, 163–180.

Galano, A. and Francisco-Marquez, M. (2009) Reactions of OOH radical with β-carotene, lycopene, and torulene: hydrogen atom transfer and adduct formation mechanisms. *J. Phys. Chem. B*, **113**, 11338–11345.

Gill, S. S. and Tuteja, N. (2010) Reactive oxygen species and antioxidant machinery in abiotic stress tolerance in crop plants. *Plant Physiol. Bioch.*, **48**, 909–930.

Gong, L., Zhang, H., Gan, X., Zhang, L., Chen, Y. et al. (2015) Transcriptome profiling of the potato (*Solanum tuberosum* L.) plant under drought stress and water-stimulus conditions. *PLoS One*, **10**, e128041.

Grabherr, M. G., Haas, B. J., Yassour, M., Levin, J. Z., Thompson, D. A. et al. (2011) Full-length transcriptome assembly from RNA-Seq data without a reference genome. *Nat. Biotechnol.*, **29**, 644–652.

Herz, S., Weber, R. W. S., Anke, H., Mucci, A., and Davoli, P. (2007) Intermediates in the oxidative pathway from torulene to torularhodin in the red yeasts *Cystofilobasidium infirmominiatum* and *C. capitatum* (Heterobasidiomycetes, Fungi). *Phytochemistry*, **68**, 2503–2511.

Hren, M., Nikolic, P., Rotter, A., Blejec, A., Terrier, N. et al. (2009) 'Bois noir' phytoplasma induces significant reprogramming of the leaf transcriptome in the field grown grapevine. *Bmc Genomics*, **10**, 460.

Iseli, C., Jongeneel, C. V., and Bucher, P. (1999) ESTScan: a program for detecting, evaluating, and reconstructing potential coding regions in EST sequences. *Proc. Int. Conf. Intell. Syst. Mol. Biol.*, 138–148.

Kang, L., Ji, C. Y., Kim, S. H., Ke, Q., Park, S. C. et al. (2017) Suppression of the β-carotene hydroxylase gene increases β-carotene content and tolerance to abiotic stress in transgenic sweetpotato plants. *Plant Physiol. Bioch.*, **117**, 24–33.

Kim, S. H., Ahn, Y. O., Ahn, M., Jeong, J. C., Lee, H. et al. (2013) Cloning and characterization of an *Orange* gene that increases carotenoid accumulation and salt stress tolerance in transgenic sweetpotato cultures. *Plant Physiol. Bioch.*, **70**, 445–454.

Kot, A. M., Blazejak, S., Gientka, I., Kieliszek, M., and Brys, J. (2018) Torulene and torularhodin: "new" fungal carotenoids for industry? *Microb. Cell Fact.*, **17**, 49.

Latha, B. V. and Jeevaratanm, K. (2012) Thirteen-week oral toxicity study of carotenoid pigment from *Rhodotorula glutinis* DFR-PDY in rats. *Indian J. of Exp. Bio.*, **50**, 645–651.

Li, B. and Dewey, C. N. (2011) RSEM: accurate transcript quantification from RNA-Seq data with or without a reference genome. *Bmc Bioinformatics*, **12**, 323.

Li, C., Zhang, N., Song, J., Wei, N., Li, B. et al. (2016) A single desaturase gene from red yeast *Sporidiobolus pararoseus* is responsible for both four- and five-step dehydrogenation of phytoene. *Gene*, **590**, 169–176.

Li, C., Zhang, N., Li, B., Xu, Q., Song, J. et al. (2017a) Increased torulene accumulation in red yeast *Sporidiobolus pararoseus* NGR as stress response to high salt conditions. *Food Chem.*, **237**, 1041–1047.

Li, D., Xie, Z., Zand, M., Fogg, T., and Dye, T. (2017b) Bon-EV: an improved multiple testing procedure for controlling false discovery rates. *Bmc Bioinformatics*, **18**, 1.

Liu, J., Zhou, Y., Luo, C., Xiang, Y., and An, L. (2016) De novo transcriptome sequencing of desert herbaceous *Achnatherum splendens* (Achnatherum) seedlings and identification of salt tolerance genes. *Genes*, **7**, 12.

Maiani, G., Periago Castón, M. J., Catasta, G., Toti, E., Cambrodón, I. G. et al. (2009) Carotenoids: Actual knowledge on food sources, intakes, stability and bioavailability and their protective role in humans. *Mol. Nutr. Food Res.*, **53**, S194–S218.

Mannazzu, I., Landolfo, S., Da Silva, T. L., and Buzzini, P. (2015) Red yeasts and carotenoid production: outlining a future for non-conventional yeasts of biotechnological interest. *World J. Microb. Biot.*, **31**, 1665–1673.

Manowattana, A., Techapun, C., Watanabe, M., and Chaiyaso, T. (2017) Bioconversion of biodiesel-derived crude glycerol into lipids and carotenoids by an oleaginous red yeast *Sporidiobolus pararoseus* KM281507 in an airlift bioreactor. *J. Biosci. Bioeng.*, **125**, 59–66.

Martin, J. A. and Wang, Z. (2011) Next-generation transcriptome assembly. *Nat. Rev. Genet.*, **12**, 671–682.

Mata-Gomez, L. C., Montanez, J. C., Mendez-Zavala, A., and Aguilar, C. N. (2014) Biotechnological production of carotenoids by yeasts: an overview. *Microb. Cell Fact.*, **13**, 12.

Miller, G., Suzuki, N., and Ciftci-Yilmaz, S. (2010) Reactive oxygen species homeostasis and signalling during drought and salinity stresses. *Plant, Cell Environ.*, **33**, 453–467.

Müller, L., Fröhlich, K., and Böhm, V. (2011) Comparative antioxidant activities of carotenoids measured by ferric reducing antioxidant power (FRAP), ABTS bleaching assay (αTEAC), DPPH assay and peroxyl radical scavenging assay. *Food Chem.*, **129**, 139–148.

Mutz, K., Heilkenbrinker, A., Lönne, M., Walter, J., and Stahl, F. (2013) Transcriptome analysis using next-generation sequencing. *Curr. Opin. Biotech.*, **24**, 22–30.

Rapaport, F., Khanin, R., Liang, Y., Pirun, M., Krek, A. et al. (2013) Comprehensive evaluation of differential gene expression analysis methods for RNA-seq data. *Genome Biol.*, **14**, R95.

Robinson, M. D., McCarthy, D. J., and Smyth, G. K. (2009) edgeR: a Bioconductor package for differential expression analysis of digital gene expression data. *Bioinformatics*, **26**, 139–140.

Saenge, C., Cheirsilp, B., Suksaroge, T. T., and Bourtoom, T. (2011) Potential use of oleaginous red yeast *Rhodotorula glutinis* for the bioconversion of crude glycerol from biodiesel plant to lipids and carotenoids. *Process Biochem.*, **46**, 210–218.

Sakaki, H., Nochide, H., Komemushi, S., and Miki, W. (2002) Effect of active oxygen species on the productivity of torularhodin by *Rhodotorula glutinis* No. 21. *J. Biosci. Bioeng.*, **93**, 338–340.

Sandmann, G., Zhu, C., Krubasik, P., and Fraser, P. D. (2006) The biotechnological potential of the al-2 gene from *Neurospra crassa* for the production of monocyclic keto hydroxy carotenoids. *BBA - Mol. Cell Biol. L.*, **1761**, 1085–1092.

Shen, C., Guo, H., Chen, H., Shi, Y., Meng, Y. et al. (2017) Identification and analysis of genes associated with the synthesis of bioactive constituents in *Dendrobium officinale* using RNA-Seq. *Sci. Rep.*, **7**, 187.

Shi, Y., Guo, J., Zhang, W., Jin, L., Liu, P. et al. (2015) Cloning of the lycopene β-cyclase gene in *Nicotiana tabacum* and its overexpression confers salt and drought tolerance. *Int. J. Mol. Sci.*, **16**, 30438–30457.

Udomchalothorn, T., Plaimas, K., Sripinyowanich, S., Boonchai, C., Kojonna, T. et al. (2017) OsNucleolin1-L expression in *Arabidopsis enhances* photosynthesis via transcriptome modification under salt stress conditions. *Plant Cell Physiol.*, **58**, 717–734.

Weber, R. W. S., Anke, H., and Davoli, P. (2007) Simple method for the extraction and reversed-phase high-performance liquid chromatographic analysis of carotenoid pigments from red yeasts (Basidiomycota, Fungi). *J. Chromatogr. A*, **1145**, 118–122.

Yang, H., Sun, M., Lin, S., Guo, Y., Yang, Y. et al. (2017) Transcriptome analysis of *Crossostephium chinensis* provides insight into the molecular basis of salinity stress responses. *PLoS One*, **12**, e187124.

Zhang, X., Liao, M., Chang, D., and Zhang, F. (2014) Comparative transcriptome analysis of the Asteraceae halophyte Karelinia caspica under salt stress. *BMC Research Notes*, **7**, 927.

Zoz, L., Carvalho, J. C., Soccol, V. T., Casagrande, T. C., and Cardoso, L. (2015) Torularhodin and torulene: bioproduction, properties and prospective applications in food and cosmetics—a review. *Braz. Arch. Biol. Technol.*, **58**, 278–288.

Zuluaga, M., Gueguen, V., Pavondjavid, G., and Letourneur, D. (2017) Carotenoids from microalgae to block oxidative stress. *BioImpacts*, **7**, 1–3.